Formation of quantized vortices in a gaseous Bose-Einstein condensate

F. Chevy, K. W. Madison, V. Bretin, and J. Dalibard
Laboratoire Kastler Brossel,
24 rue Lhomond, 75005 Paris, France.

April 7, 2002

Abstract

Using a focused laser beam we stir a Bose-Einstein condensate confined in a magnetic trap. When the stirring frequency lies near the transverse quadrupolar mode resonance we observe the nucleation of vortices. When several vortices are nucleated, they arrange themselves in regular Abrikosov arrays, and in the limit of large quantum number the lattice structure is shown to produce a quantum velocity field approaching that for classical, rigid body rotation. Using a percussive excitation of the condensate, we measure the angular momentum of the condensate with vortices present and study the nucleation band as a function of the stirring intensity and geometry. We find that with only quadratic terms in the rotating perturbation the nucleation band is located around the quadrupolar resonance and has a width that increases with the strength of the stirring perturbation. However, when the potential includes cubic terms, the nucleation band broadens to include the hexapolar resonance as well. The results presented here demonstrate that the nucleation of vortices in the case of a harmonically trapped BEC is driven by the resonant excitation of the rotating quadrupolar mode, or by higher order rotating surface modes when the rotating perturbation includes the corresponding terms.

1

1   Introduction

Superfluidity, originally discovered and studied in the context of superconductors and later in the system of superfluid liquid Helium, is a hallmark property of interacting quantum fluids and encompasses a whole class of fundamental phenomena [1, 2]. With the achievement of Bose-Einstein condensation (BEC) in laser-precooled atomic gases [3, 4, 5, 6], it became possible to study these phenomena in an extremely dilute quantum fluid, thus helping to bridge the gap between theoretical studies, only tractable in dilute systems, and experiments.

One striking consequence of superfluidity is the response of a quantum fluid to a rotating perturbation. In contrast to a normal fluid, which at thermal equilibrium will rotate like a solid body with the perturbation, a superfluid will not circulate unless the frequency of the perturbation is larger than some critical frequency, analogous to the critical velocity [1]. Moreover, when the superfluid does circulate, it can only do so by forming vortices in which the condensate density vanishes and for which the velocity field flow evalutated around a closed contour is quantized. Due to their mutual repulsion these vortices can cristallize into a regular lattice known in condensed matter as an Abrikosov lattice [7].

The observation of superfluid phenomena in a dilute BEC has been the subject of much experimental and theoretical work during the last two years. A first class of study has been performed at MIT and consists in measuring the energy deposited in the condensate by a moving "object" (a hole created by a repulsive laser)[8]. The second class of study is based on specific oscillation patterns of the condensate, in particular the *scissors mode*. This was studied theoretically by D. Guéry-Odelin and S. Stringari [9] and investigated experimentally by the Oxford group [10]. Finally another clue for superfluidity is related to the behavior of vortices. Using a "phase printing method", the Boulder group has created a vortex in a double component condensate with one component standing still at the center of a magnetic trap and the other component in quantized rotation around the first one [11]. In subsequent experiments this group also succeeded in emptying the core of the double component vortex [12], and showed that vortex rings can form as decay products of a dark soliton [13].

In our work in Paris, we have studied the response of a trapped, single component condensate to a rotating perturbation created by a stirring laser beam. When the stirring frequency lies near the transverse quadrupolar mode resonance we observe the nucleation of vortices [14]. We also find that multiple vortices can be nucleated and that they spontaneously arrange themselves into regular

Abrikosov lattices containing up to 14 vortices for our experimental condition [15]. A similar observation has been made quite recently at MIT with a larger sodium condensate, in which large arrays of vortices (up to 150) have been nucleated [16].

We observe that in accordance with the correspondence principle, the large quantum number limit yields a quantum velocity field that approaches that for classical, rigid body rotation. Using a percussive excitation of the condensate, we measure the angular momentum of the condensate with vortices present and study the nucleation band as a function of the stirring intensity and geometry [17]. We find that with only quadratic terms in the rotating perturbation the nucleation band is located at the quadrupolar resonance and has a width that depends on the strength of the stirring perturbation. However, when the potential includes cubic terms, the nucleation band broadens to include the hexapolar resonance as well. The results presented here demonstrate that the nucleation of vortices in the case of a harmonically trapped BEC is driven by the resonant excitation of the rotating quadrupolar mode, or by higher order rotating surface modes when the rotating perturbation includes the corresponding terms.

Our experiment is a direct transposition to atomic gases of the famous "rotating bucket experiment" performed with liquid helium. In § 2 we briefly recall some essential results obtained with this experimental scheme for superfluid He. We then turn in § 3 to the description of our experimental setup. The observation of single and multiple vortices is presented in § 4 where we also discuss the lattice structure. Finally, in § 5 we discuss the measurement of the angular momentum of the condensate as a function of the stirring intensity and geometry.

2 The rotating bucket experiment

Consider a superfluid placed in a bucket rotating at angular frequency Ω (fig. 1). If Ω is smaller than a critical value Ω_c, the superfluid will not circulate, which is is a direct manifestation of superfluidity. The existence of this critical angular frequency is analogous to that of a critical linear flow velocity below which the condensate exhibits viscous free behaviour. Here the slow motion of the rough walls of the bucket does not rotate the superfluid. As shown by Landau, superfluidity is a direct consequence of repulsive interactions which gives rise to a phonon-like dispersion relation for the lowest lying excitations [1].

When Ω is increased beyond the critical frequency Ω_c the superfluid is set

into motion. As pointed out by Onsager [18] and Feynman [19] the corresponding velocity field is subject to very strong constraints due to its quantum nature. Consider the macroscopic wave function $\psi(\mathbf{r})$ describing the state of the superfluid. It can be written:

$$\psi(\mathbf{r}) = \sqrt{\rho(\mathbf{r})} \, \exp i\theta(\mathbf{r}) \, , \tag{1}$$

where $\rho(\mathbf{r})$ is the superfluid density. The corresponding velocity field is given by:

$$\mathbf{v}(\mathbf{r}) = \frac{\hbar}{M}\nabla\theta(\mathbf{r}) \, . \tag{2}$$

where M is the mass of one atom. From Eq. (2) it is clear that the circulation of the velocity along any closed contour is quantized as a multiple of h/M:

$$\oint \mathbf{v} \cdot d\mathbf{r} = n\frac{h}{M} \qquad \text{where } n \text{ is an integer.} \tag{3}$$

Just above Ω_{c}, the superfluid wave function has a singular line or *vortex line*, along which the density is zero. On any closed path going around this line the phase of the wave function varies continuously from 0 to 2π.

It is worth emphazing that these vortices are universal structures associated with a circulating quantum flow. Besides superfluid liquid helium, other large quantum systems such as neutron stars and superconductors support quantized vortices. In the latter case the rotation vector is induced by an applied magnetic field which modifies the motion of the charges, and the quantization of the circulation of the velocity field results in magnetic flux quantization.

For a rotating frequency Ω notably larger than Ω_{c}, several vortex lines can be generated, and they form a regular triangular lattice. Such regular lattices were orginally predicted to occur in type-II superconductors by Abrikosov [7] and were subsequently observed experimentally by imaging with an electron microscope small ferromagnetic particles which when scattered on the surface of a superconductor in a magnetic field accumulate at the flux line exit points [20, 21]. Evidence of vortex lattice arrangements in liquid helium was demonstrated by trapping electrons at the core of each vortex and then accelerating the electrons along the vortex lines to a phosphorus screen [22].

3 The experimental setup

Our experiment is performed with a ^{87}Rb gaseous condensate (fig. 2) confined in an Ioffe-Pritchard magnetic trap. The magnetic trap is an axisymmetric harmonic potential:

$$U(\mathbf{r}) = \frac{1}{2}M\omega_\perp^2(x^2 + y^2) + \frac{1}{2}M\omega_z^2 z^2 \ , \tag{4}$$

with a transverse frequency $\omega_\perp/2\pi$ varying from 90 to 225 Hz and an axial frequency $\omega_z/2\pi$ between 10 Hz and 12 Hz. The condensate is cigar-shaped, with a length of $\sim 110\ \mu$m and a diameter of 7 μm for 2×10^5 atoms and a trapping frequency of 170 Hz.

The stirring of the condensate is provided by a focused 500 μW laser beam of wavelength 852 nm and waist $w_0 = 20\ \mu$m, whose motion is controlled using acousto-optic deflectors. This laser propagates along the axis of the cigar, and it toggles back and forth very rapidly between two symmetric positions 8 μm from the center of the condensate. The toggling frequency is chosen to be 100 kHz which is much larger than both ω_z and $\omega_\perp$. It creates for the atoms an average dipole potential which is anisotropic in the xy plane (fig. 2). This potential contains only even terms because of symmetry and the leading order term is:

$$\delta U(\mathbf{r}) = \frac{1}{2}M\omega_\perp^2(\epsilon_X X^2 + \epsilon_Y Y^2) \tag{5}$$

where ϵ_X and ϵ_Y depend on the intensity, waist, and the spacing of the stirring beams. Using the acousto-optic deflectors, the XY axes are rotated at an angular frequency Ω producing a rotating harmonic trap characterized by the three trap frequencies $\omega_{X,Y}^2 = \omega_\perp^2(1 + \epsilon_{X,Y})$ and ω_z. Using

$$X = x\cos(\Omega t) + y\sin(\Omega t) \qquad Y = -x\sin(\Omega t) + y\cos(\Omega t) \tag{6}$$

we can write the total potential in the rotating and in the lab frame as:

$$\begin{aligned}(U + \delta U)\,(\mathbf{r}) &= \frac{1}{2}M(\omega_X^2 X^2 + \omega_Y^2 Y^2) + \frac{1}{2}M\omega_z^2 z^2 \tag{7}\\ &= \frac{1}{2}M\bar{\omega}_\perp^2(x^2 + y^2) + \frac{1}{2}M\omega_z^2 z^2 \\ &\quad + \frac{1}{2}M\,\epsilon\,\bar{\omega}_\perp^2\left((x^2 - y^2)\cos(2\Omega t) + 2xy\sin(2\Omega t)\right) \tag{8}\end{aligned}$$

where we have set

$$\bar{\omega}_\perp = \sqrt{(\omega_X^2 + \omega_Y^2)/2} \qquad\qquad \epsilon = (\omega_X^2 - \omega_Y^2)/(\omega_X^2 + \omega_Y^2) \ . \qquad (9)$$

This potential is stationary in the rotating frame (eq. (7)) and oscillates periodically at frequency 2Ω in the laboratory frame (eq. (8)). The stirring frequency Ω is usually chosen in the interval $(0, \omega_\perp)$. At the upper value of this interval, the centrifugal force equals the transverse restoring force of the trap. A dynamical instability of the center of mass motion of the condensate occurs when Ω lies in the interval $[\omega_Y, \omega_X]$ (assuming $\epsilon_Y < \epsilon_X$). The steepness of this parametric resonance provides a very accurate measurement of the trap frequencies ω_X and ω_Y.

The experimental procedure begins with the loading of 10^8 ^{87}Rb atoms into a magneto-optic trap from a cold atomic jet produced by a separate magneto-optic trap loading from a room temperature vapor [23]. We then precool the atoms to 10 μK in an optical molasses and transfer them into the magnetic trap. The generation of a condensate in the pure magnetic potential is provided by a radio-frequency (rf) evaporation ramp lasting 25 s. The atomic cloud reaches the critical temperature $T_c \sim 500$ nK with an atom number of $\sim 2.5\,10^6$. The evaporation is continued below T_c to a temperature of or below 100 nK at which point 3 (± 0.7) 10^5 atoms are left in the condensate. The rf frequency is then set 20 kHz above $\nu_{\mathrm{rf}}^{\min}$, the rf frequency which corresponds to the bottom of the magnetic potential. This rf drive is kept present in order to hold the temperature approximately constant. At this point, the stirring laser is switched on and the condensate is allowed to evolve in the combined magnetic and optical potential for a controlled duration. Finally, the stirring potential is extinguished adiabatically (in a time long compared to $\omega_\perp^{-1}$) and the condensate density profile along the stirring axis is measured to detect the presence of vortices.

We now address the question of the vortex visibility. In a fluid of density ρ, the radius of the vortex core is determined by the healing length $\xi = (8\pi\rho a)^{-1/2}$, where a is the scattering length characterizing the two-body interactions in the ultra-low temperature regime [1]. For our experimental conditions, $\xi \sim 0.2$ μm, which is too small to be observed optically with resonant light at 780 nm. Fortunately this size can be expanded using a time-of-flight technique [24, 25, 26]. When we release the atomic cloud from the magnetic trap and let it expand for a duration T, the transverse dimensions of the condensate and of the vortex core are increased by a factor of $(1 + \omega_\perp^2 T^2)^{1/2} \sim 35$ for $T = 27$ ms and a transverse

trapping frequency of $\omega_\perp/2\pi = 170$ Hz. The detection of the expanded condensate density profile is then performed by imaging the absorption of a resonant laser beam propagating along the z axis.

4 Single and multiple vortices

We now discuss the results of this experiment. When the stirring frequency is below a threshold frequency Ω_{th} depending on the stirring ellipticity, no modification of the condensate is observed. Just above this critical frequency (within 1 or 2 Hz), a density dip appears at the center of the cloud, with a reduction of the optical thickness at this location which reaches 50% (fig. 3).

When we stir the condensate at a frequency higher than Ω_{th}, more vortices are nucleated (fig. 4). The maximum number of vortices generated in this experiment depends on the transverse oscillation frequency $\bar\omega_\perp$. For a relatively tight trap ($\bar\omega_\perp/2\pi = 225$ Hz), we have observed up to 4 vortices [14]. When we used a less confining trap ($\bar\omega_\perp/2\pi \sim 100$ Hz), we obtained configurations where more vortices were present [15]. In fig. 4 we show images of vortex lattices generated in a trap with $\bar\omega_\perp/2\pi = 103$ Hz, where we obtained configurations with up to 14 clearly visible vortices.

The existence of regular vortex lattices is a consequence of the balance between the repulsive interaction between two vortex lines and the restoring force that acts on a vortex line centering it on the condensate (see fig. 3). Although the lowest energy configuration is a triangular lattice, the square pattern is only slightly higher in energy and is sometimes observed (see fig. 4) [27, 2].

In the large vortex number limit, the density of vortices can be deduced from the *correspondence principle*. In this limit, the coarse grain average (on a scale larger than the distance between two vortices) of the quantum velocity field should be the same as that for classical, rigid-body rotation $\mathbf{v} = \mathbf{\Omega} \times \mathbf{r}$ [19].

In order to recover this linear variation of the velocity field with $\mathbf{r}$, the distance from the rotation axis, the surface density of vortices ρ_v must be uniform. The circulation of the velocity field $\oint \mathbf{v} \cdot d\mathbf{r}$ on a circle of radius R centered on the condensate is then $\mathcal{N}(R)\, h/M$, where $\mathcal{N}(R) = \rho_{\mathrm{v}} \pi R^2$ is the number of vortices contained in the circle (see eq. (3)). This is equivalent to the rigid body circulation $2\pi R^2 \Omega$ if

$$\rho_{\mathrm{v}} = \frac{2M\Omega}{h} \ .\tag{10}$$

Consider for instance the vortex lattice shown in fig. 5, which contains $\mathcal{N} = 12$ visible vortices. The circle drawn on the edge of the condensate has a radius 80 μm after the time-of-flight expansion, i.e. $R = 5$ μm before expansion (using the expansion factor given above $\sqrt{1 + \omega_\perp^2 T^2}$). The stirring frequency in this experiment was $\Omega/2\pi = 77$ Hz, which yields the ratio between the average velocity $\bar{v}$ on the circle and the velocity v_r corresponding rigid body rotation:

$$\frac{\bar{v}}{v_r} = \frac{\mathcal{N}\hbar}{M\Omega R^2} \simeq 0.7 \ . \tag{11}$$

This shows that the coarse grain average velocity field of the condensate shown in fig. 5 is close that of a rigid body rotating at the stirring frequency Ω.

5 Vortex nucleation versus stirring intensity and geometry

After this qualitative observation of vortex nucleation and lattice structure, we turn to a more quantitative observation of vortex nucleation provided by the measurement of the angular momentum per particle in a condensate with vortices. For this purpose we employ a theoretical result derived by F. Zambelli and S. Stringari [28]. These authors have studied the two transverse quadrupole modes of a cylindrically symmetric condensate, corresponding respectively to excitations with angular momentum $m = 2$ and $m = -2$. Because of symmetry for a condensate at rest, these two modes have the same frequency. However, for a condensate with a net circulation, the degeneracy is lifted, and the frequency difference between the two modes is related to the average angular momentum per particle $\langle L_z \rangle$ and to the transverse size of the condensate $\langle r_\perp^2 \rangle$:

$$\omega_+ - \omega_- = \frac{2\langle L_z \rangle}{M\langle r_\perp^2 \rangle} \tag{12}$$

The measurement of the difference $\omega_+ - \omega_-$ is performed by looking at the transverse quadrupolar oscillation of the condensate which is produced by a superposition of both the $m = 2$ and $m = -2$ excitations [17, ?]. In the absence of vortices $\omega_+ = \omega_-$ and the oscillation occurs along fixed axes. However, if ω_+ and ω_- differ, the axes of the quadrupolar oscillation precess, and the precession frequency is $\dot{\theta} = (\omega_+ - \omega_-)/4$.

To study the angular momentum $\langle L_z \rangle$ of the condensate, we first stir it with the rotating laser potential. We then excite the transverse quadrupolar oscillation using again the dipole potential created by the stirring laser but now with a fixed basis $(x, y = X, Y)$. This potential is applied to the atoms for a duration of 0.3 ms, which is short compared to the quadrupolar oscillation period $2\pi/\omega_{\text{QP}}$ ($\omega_{\text{QP}} = \sqrt{2}\,\omega_\perp$). We then let the atomic cloud oscillate freely in the pure magnetic trap for an adjustable period τ, between 0 and 8 ms, after which we perform the time-of-flight + absorption imaging sequence. A typical result is shown in fig. 6. It displays three images taken 1, 3 and 5 ms after the quadrupolar excitation of a condensate with a vortex present. The precession of the quadrupolar axes is clearly visible and has an angular velocity $\dot{\theta} = 5.9$ degrees/ms. For this set of pictures, the transverse trapping frequency is 172 Hz and the *in situ* transverse size of the condensate (inferred from the size measured after time-of-flight and the expansion factor $(1 + \omega_\perp^2 T^2)^{1/2}$) is $\langle r_\perp^2 \rangle^{1/2} = 2.0$ μm. From $\dot{\theta}$ and $\langle r_\perp^2 \rangle$ we deduce the value $L_z = 1.2$ (± 0.1) $\hbar$ from the data shown in fig. 6. A similar observation has also been made in Boulder [29]. This measurement is analogous to the experiment performed with superfluid liquid helium by Vinen in which he detected a single quantum of circulation in rotating He II by measuring the frequencies of two opposing circular vibrational modes of a thin wire placed at the center of the rotating fluid [30].

We have repeated this angular momentum measurement for various stirring frequencies and ellipticities, and the results for two intensities are shown in fig. 7. Both plots display a region where vortices are nucleated, and the more intense the stirring anisotropy the wider is this region. For very small stirring intensities, this region has a width of only a few Hz, and it is centered on a stirring frequency $2\pi \times 125$ Hz. This corresponds to the situation where the time-dependent perturbation in the lab frame oscillating at frequency 2Ω (see Eq. (8)) is resonant with the quadrupole mode at frequency ω_{QP}. In other words, the resonance observed for very low stirring intensities occurs when Ω is close to the quadrupolar rotational resonance $\omega_{\text{QP}}/2$, which is equal to $\sqrt{2}\,\bar{\omega}_\perp/2 \simeq 2\pi \times 122$ Hz in the Thomas Fermi limit [31]. This coincidence and the observation of very strong BEC ellipticities during the first tens of milliseconds of stirring indicates that the mechanism for vortex nucleation involves the resonant excitation of the rotating quadrupole mode [32]. The details of how the rotating quadrupole mode leads to the nucleation of vortices after its excitation by the rotating potential is beyond the scope of this paper, and they are discussed in [33].

We note here that the percussive measurement of L_z is performed 200 ms

after the stirring anisotropy is switched off. This delay is (i) short compared to the vortex lifetime [14] and (ii) long compared to the measured relaxation time (~ 25 ms) of the aforementioned ellipticity of the condensate excited by the stirring. Therefore a nonzero value of L_z is a clear signature of vortex nucleation.

The role of the resonant excitation of the transverse quadrupole mode in vortex nucleation suggests the possibility that vortices might be created by exciting transverse collective modes of higher angular momenta, m, at their resonant rotational frequencies $\Omega_m \simeq \bar{\omega}_\perp / \sqrt{m}$ [31, 32, 34, 16]. In order to investigate this possibility, the stirring potential must include non-negligible terms of higher order in X and Y. Although the two-beam stirring potential whose dominant term is given in Eq. 5 contains in principle all even orders, their magnitude is too small in practice to be relevant for $m \geq 4$. Using a single-beam stirring potential (i.e. suppressing the toggling motion) the odd terms are no longer canceled. To leading order, the resulting potential then contains the same quadratic term as before (Eq. 5) as well as a linear and cubic term. Although the linear term can directly excite the center of mass motion of the condensate, a time dependent displacement of the center of a harmonic trap produces only a movement of the center of mass of the wavefunction and no deformation even in the presence of interactions [35].

The presence of the cubic term, however, allows for the resonant excitation of the rotating hexapole mode ($m = 3$) at a frequency of $\bar{\omega}_\perp / \sqrt{3} \simeq 0.58\,\bar{\omega}_\perp$. fig. 8 shows the results of an angular momentum measurement for various stirring frequencies with both a two beam and single beam stirring scheme where $\bar{\omega}_\perp / 2\pi = 100$ Hz. In the case of the single stirring beam, the nucleation band includes the quadrupolar resonance centered at 71 Hz and extends beyond this down to 45 Hz including the hexapole resonance at 58 Hz.

The vortex nucleation peak near 35 Hz present on the two curves of fig. 8 is due to the difference of the diffraction efficiencies of the two acousto-optic deflectors controlling the the stirring beam position. This slight difference of efficiency creates a small modulation of the intensity of the stirring potential at twice the stirring frequency. This intensity modulation therefore modulates the transverse trap frequency at 70 Hz, and this modulation can excite parametrically the quadrupolar resonance. We indeed observe in this case the excitation of the rotating quadrupole mode and its subsequent decay into vortex states as before. We emphasize that nucleation at this low frequency is not relevant in the usual study of vortex nucleation, since in the rotating frame the potential is no longer stationary: actually it is not stationary in any frame!

6   Conclusions

In conclusion we report on a rotating bucket experiment performed with a gaseous condensate. We observe (i) that there exists a frequency band in which vortices can be nucleated; (ii) that for a quadratic rotating perturbation this band is centered on a critical frequency Ω_c identified with the rotating quadrupole mode; (iii) that the width of this band can be significantly increased by changing the stirring beam potential to excite surface excitations of higher order, and (iv) that multiple vortices can be nucleated and will arrange themselves into regular Abrikosov lattices for which, in the large quantum number limit, the velocity field approaches that for classical, rigid body rotation. The results presented here demonstrate that the nucleation of vortices in the case of a harmonically trapped BEC is related to the resonant (dynamical) excitation of the rotating quadrupole mode and its subsequent decay into a vortex state. This nucleation mechanism is different from the scenarii expected from previous theoretical work which concentrated on the study of thermodynamical instabilities. Indeed one predicts in this case a critical nucleation frequency much lower than what is observed, and a nucleation region extending to $\bar{\omega}_\perp$ [36, 37, 38, 39, 40, 41, 42, 43, 44, 45, 46, 47].

The dynamical instability of the condensate in presence of a small rotating anisotropy has been studied by numerically integrating the zero temperature Gross-Pitaevski equation and found to produce states with nonzero angular momentum [48, 49]. We have recently studied this issue experimentally and clarified the excitation and decay routes of the rotating quadrupole mode which lead to vortex nucleation [33]. We now plan to pursue a detailed investigation of the possible bending of vortex lines [50] and of the decay of vortices, which is relevant to the physics of rotating neutron stars [51, 52].

References

[1] E.M. Lifshitz and L. P. Pitaevskii, *Statistical Physics, Part 2*, chap. III (Butterworth-Heinemann, 1980).

[2] R.J. Donnelly, *Quantized Vortices in Helium II*, (Cambridge, 1991).

[3] M. H. Anderson, J. Ensher, M. Matthews, C. Wieman, and E. Cornell, Science **269**, 198 (1995).

[4] C. C. Bradley, C. A. Sackett, and R. G. Hulet, Phys. Rev. Lett. **78**, 985 (1997); see also C. C. Bradley, C. A. Sackett, J. J. Tollett, and R. G. Hulet, Phys. Rev. Lett. **75**, 1687 (1995).

[5] K. B. Davis, M.O. Mewes, N. Van Druten, D. Durfee, D. Kurn, and W. Ketterle, Phys. Rev. Lett. **75**, 3969 (1995).

[6] D. Fried, T. Killian, L. Willmann, D. Landhuis, S. Moss, D. Kleppner, and T. Greytak, Phys. Rev. Lett. **81**, 3811 (1998).

[7] A. A. Abrikosov, JETP **32**, 1442 (1957)

[8] C. Raman, M. Köhl, R. Onofrio, D. S. Durfee, C. E. Kuklewicz, Z. Hadzibabic, and W. Ketterle, Phys. Rev. Lett. **83**, 2502 (1999); A.P. Chikkatur, A. Gorlitz, D.M. Stamper-Kurn, S. Inouye, S. Gupta, and W. Ketterle, Phys. Rev. Lett. **85**, 483 (2000); R. Onofrio, C. Raman, J. M. Vogels, J. Abo-Shaeer, A. P. Chikkatur, and W. Ketterle, Phys. Rev. Lett. **85**, 2228 (2000).

[9] D. Guéry-Odelin and S. Stringari, Phys. Rev. Lett. **83**, 4452 (1999).

[10] O. M. Maragò, S. A. Hopkins, J. Arlt, E. Hodby, G. Hechenblaikner, and C. J. Foot, Phys. Rev. Lett. **84**, 2056 (2000).

[11] M. R. Matthews, B. P. Anderson, P. C. Haljan, D. S. Hall, C. E. Wieman, and E. A. Cornell, Phys. Rev. Lett. **83**, 2498 (1999).

[12] B. P. Anderson, P. C. Haljan, C. E. Wieman, and E. A. Cornell, Phys. Rev. Lett. **85**, 2857 (2000).

[13] B. P. Anderson, P. C. Haljan, C. A. Regal, D. L. Feder, L. A. Collins, C. W. Clark, and E. A. Cornell, Phys. Rev. Lett. **86**, 2926 (2001).

[14] K. W. Madison, F. Chevy, W. Wohlleben, and J. Dalibard, Phys. Rev. Lett. **84**, 806 (2000).

[15] K. W. Madison, F. Chevy, W. Wohlleben, and J. Dalibard, J. Mod. Opt. **47**, 2715 (2000) (cond-mat/ 0004037).

[16] J. R. Abo-Shaeer, C. Raman, J. M. Vogels, and W. Ketterle, published online March 22, 2001; 10.1126/science.1060182 (Science Express Research Articles).

[17] F. Chevy, K. Madison, and J. Dalibard, Phys. Rev. Lett. **85**, 2223 (2000).

[18] L. Onsager, Nuovo Cimento **6**, suppl. 2, 249 (1949).

[19] R.P. Feynman, in "Progress in Low Temperature Physics", vol. 1, ed. by C. J. Gorter, North-Holland, Amsterdam.

[20] H. Träuble and U. Essmann, J. Appl. Phys. **25**, 273 (1968).

[21] N. V. Sarma, Philos. Mag. **17**, 1233 (1968).

[22] E. J. Yarmchuk, M. J. V. Gordon, and R. E. Packard, Phys. Rev. Lett. **43**, 214 (1979).

[23] W. Wohlleben, F. Chevy, K. W. Madison, and J. Dalibard, physics/0103085.

[24] Y. Castin and R. Dum, Phys. Rev. Lett. **77**, 5315 (1996).

[25] E. Lundh, C. J. Pethick, and H. Smith, Phys. Rev. A **58**, 4816 (1998).

[26] F. Dalfovo and M. Modugno, Phys. Rev. A 61, 023605 (2000).

[27] V. K. Tkachenko, Soviet. Phys. JETP **22**, 1282 (1966).

[28] F. Zambelli and S. Stringari, Phys. Rev. Lett. **81**, 1754 (1998).

[29] P. C. Haljan, B. P. Anderson, I. Coddington, E. A. Cornell, Phys. Rev. Lett. **86**, 2922 (2001).

[30] W. F. Vinen, Nature **181**, 1524 (1958) and Proc. Roy. Soc. A **260**, 218 (1961).

[31] Although a given surface excitation of angular momentum m has an energy of $\hbar\sqrt{m}\,\bar{\omega}_\perp$ (see S. Stringari, Phys. Rev. Lett. **77**, 2360 (1996)), because it has an m-fold rotational symmetry, it is resonantly excited by a perturbation rotating at a frequency of $\Omega = \sqrt{m}\,\bar{\omega}_\perp/m = \bar{\omega}_\perp/\sqrt{m}$.

[32] F. Dalfovo and S. Stringari, Phys. Rev. A **63**, 011601(R).

[33] K. W. Madison, F. Chevy, V. Bretin, and J. Dalibard, to appear in Phys. Rev. Lett. (cond-mat/ 0101051).

[34] R. Onofrio, D. S. Durfee, C. Raman, M. Köhl, C. E. Kuklewicz, and W. Ketterle, Phys. Rev. Lett. **84**, 810 (2000).

[35] J. F. Dobson, Phys. Rev. Lett. **73**, 2244 (1994).

[36] G. Baym and C.J. Pethick, Phys. Rev. Lett. **76**, 6 (1996).

[37] F. Dalfovo and S. Stringari, Phys. Rev. A **53**, 2477 (1996).

[38] S. Sinha, Phys. Rev. A **55**, 4325 (1997).

[39] E. Lundh, C. J. Pethick, and H. Smith, Phys. Rev. A **55**, 2126 (1997).

[40] F. Dalfovo, S. Giorgini, M. Guilleumas, L. Pitaevskii, and S. Stringari, Phys. Rev. A **56**, 3840 (1997).

[41] A. Fetter, J. Low. Temp. Phys. **113**, 189 (1998).

[42] D. L. Feder, C. W. Clark, and B. I. Schneider, Phys. Rev. Lett. **82**, 4956 (1999).

[43] Y. Castin and R. Dum, Eur. Phys. J. D. **7**, 399 (1999).

[44] T. Isoshima, K. Machida, Phys. Rev. A **60**, 3313 (1999).

[45] J. Garcia-Ripoll and Victor M. Perez-Garcia, Phys. Rev. A **60**, 4864 (1999).

[46] A. Svidzinsky and A. Fetter, J. Phys. Cond. Mat. **13**, R135 (2001).

[47] D. L. Feder, C. W. Clark, and B. I. Schneider, Phys. Rev. A **61**, 011601(R) (1999).

[48] D. Feder, A. Svidzinsky, A. Fetter, and C. Clark, Phys. Rev. Lett. **86**, 564 (2001).

[49] S. Sinha and Y. Castin, cond-mat/0101292 and private communication.

[50] J. Garcia-Ripoll and Victor M. Perez-Garcia, Phys. Rev. A **63**, 041603(R).

[51] P. Fedichev and G. Shlyapnikov, Phys. Rev. A **60**, R1779 (1999).

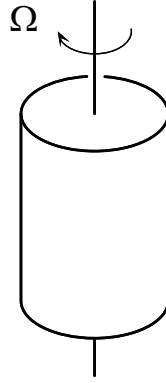[52] P. O. Fedichev and A. E. Muryshev, cond-mat/ 0004264.
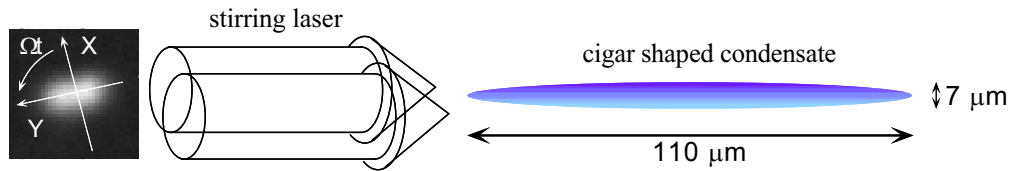
Figure 1: The rotating bucket experiment.

Figure 2: The cigar-shaped condensate is stirred using the dipole potential created by a laser "spoon". The laser waist is 20 μm; its axis is toggled between two symmetric positions about the trap axis, separated by 16 μm. The laser intensity profile averaged after this toggling is displayed on the left of the figure. The resulting anisotropic potential is then rotated at the stirring frequency Ω.
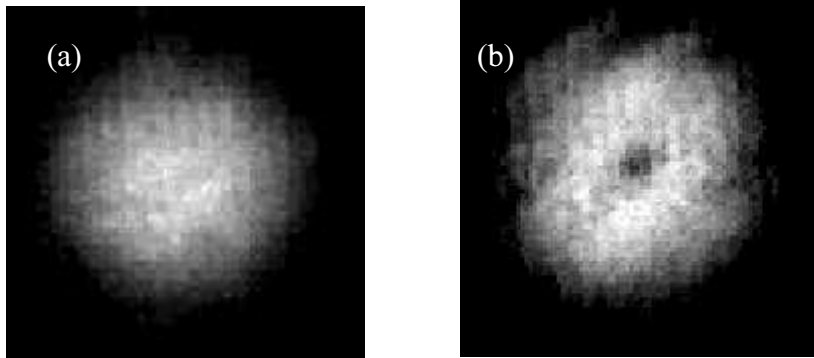
Figure 3: Density profile after a time-of-flight expansion of a Bose-Einstein condensate stirred below (left) and above (right) the threshold frequency for nucleating a vortex. $\Omega/2\pi = 145$ Hz and 152 Hz for the left and the right column respectively. The number of atoms is $N = 1.4 \times 10^5$, the temperature is below 80 nK and $\Omega_{\text{th}}/2\pi = 147$ Hz.
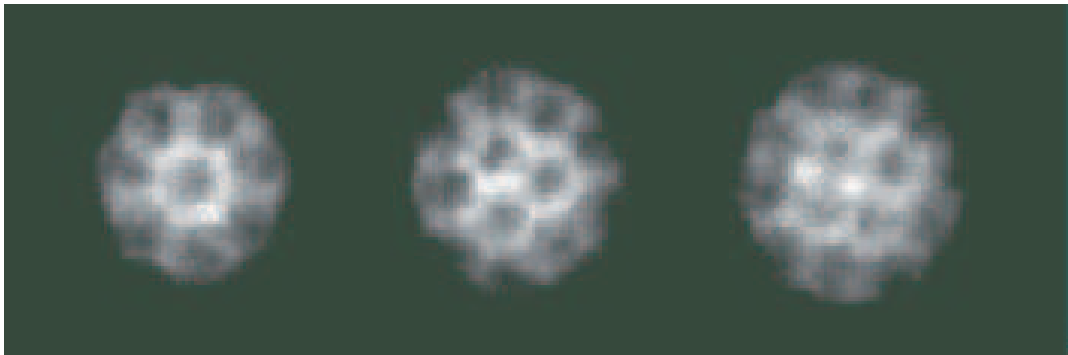

Figure 4: Arrays of vortices obtained in a magnetic trap with $\bar{\omega}_\perp/2\pi = 103$ Hz and $\Omega/2\pi = 77$ Hz. For large number of vortices, although the lowest energy configuration is a triangular lattice (middle image), the square pattern is only slightly higher in energy and is sometimes observed (right image).
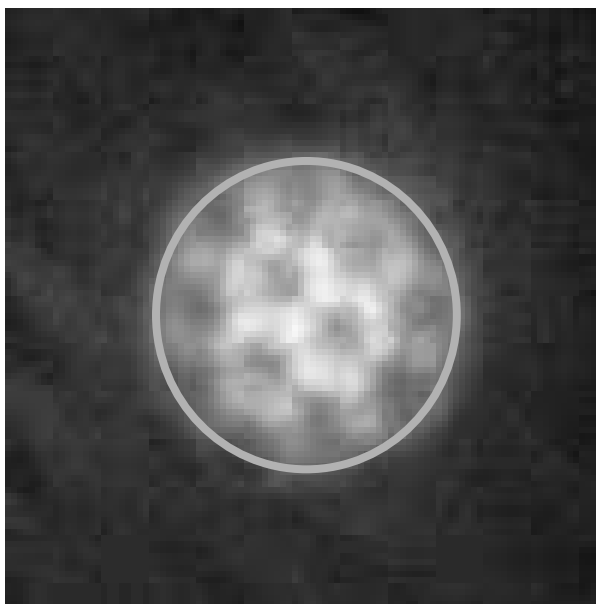
Figure 5: Array of $\mathcal{N} = 12$ vortices obtained in a magnetic trap with $\bar{\omega}_{\perp}/2\pi =$ 103 Hz and $\Omega/2\pi = 77$ Hz. The circulation of the velocity field on the circle is given by $\mathcal{N}h/m$, and is comparable with the one expected from rigid body rotation (see text).
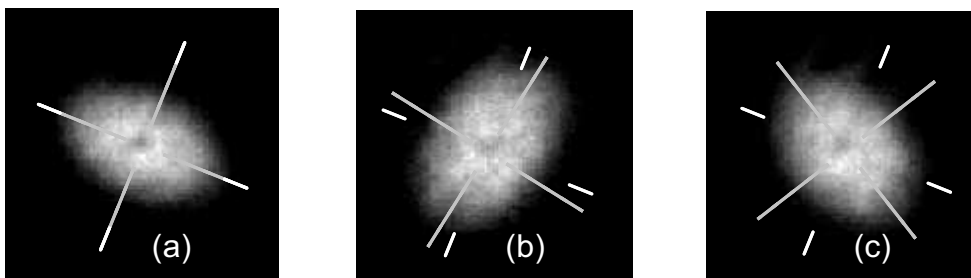

Figure 6: Transverse quadrupolar oscillations of a condensate with $N \sim 3.7 \times 10^5$ atoms and $\omega_{\perp}/2\pi = 171$ Hz. The stirring frequency is 120 Hz, slightly above the vortex nucleation threshold $\Omega_{\text{th}}/2\pi = 115$ Hz. For a,b,c: the images were taken $\tau = 1, 3, 5$ ms after the excitation of the quadrupolar oscillation. The fixed axes indicate the excitation basis and the rotating ones the condensate axes. A single vortex is visible at the center of the condensate.
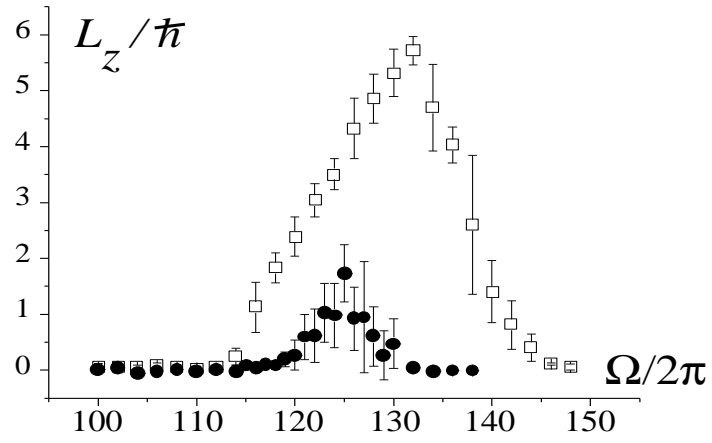
Figure 7: Angular momentum per particle of the condensate L_z deduced from Eq. (12) as a function of the stirring frequency Ω and ellipticity ϵ. ($\bullet$: $\epsilon = 0.010 \pm 0.002$; $\square$: $\epsilon = 0.019 \pm 0.004$). $\omega_\perp/2\pi = 172$ Hz and $N = 2.5 \times 10^5$ atoms.
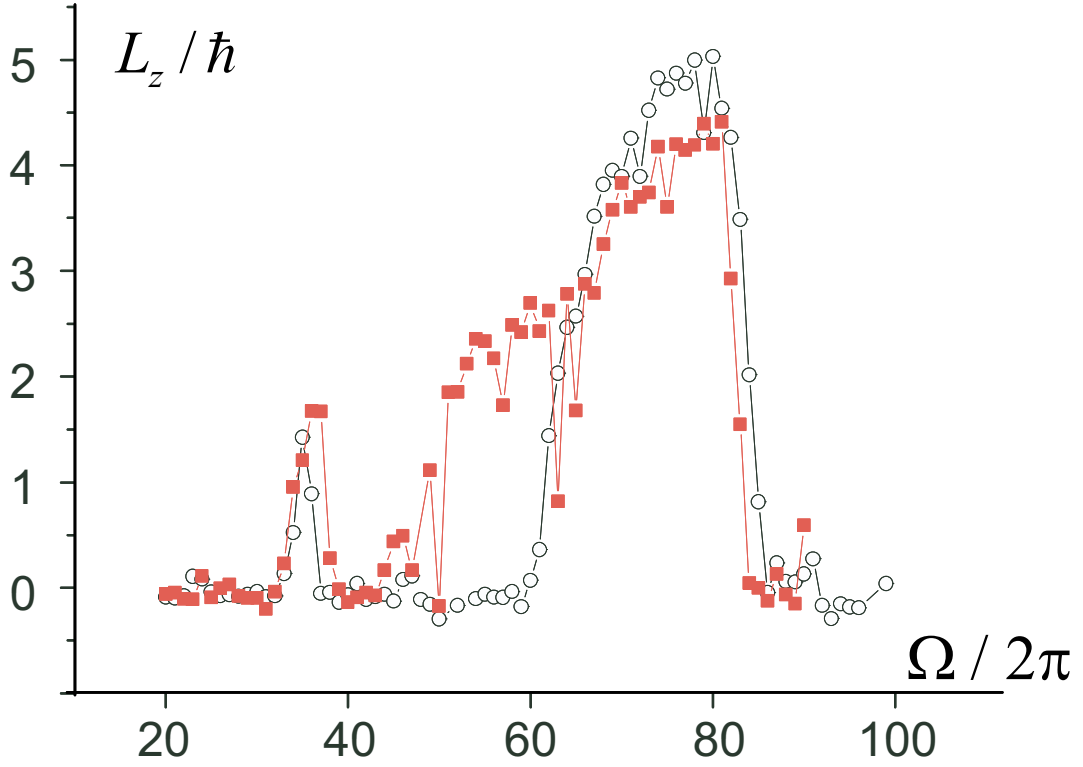
Figure 8: Angular momentum per particle versus stirring frequency for two different geometries of stirring potentials ($\bar{\omega}_\perp/2\pi = 100$ Hz). The nucleation band with the usual two-spot configuration is shown by the hollow circles ∘ and the results with a single spot are shown by the filled squares ■. In the latter case, because the potential contains terms of order three in X and Y, the nucleation range increases due to the hexapolar resonance located at 58 Hz. The nucleation peak near 35 Hz which occurs for both stirring potentials corresponds to a rotating quadrupolar resonance excited by an (unintentional) intensity modulation of the stirring potential at twice the stirring frequency (see text).